Proceedings of the 2025 SICE Festival with Annual Conference
September 9-12, 2025, Chiang Mai, Thailand

Fractional Integral Terminal Sliding Mode Control for Servo Motor Systems in Phenotyping Robot in Precision Agriculture

Watchara Jamnuch[1†], Panya Lao-anantana[2], Natthawut Chinthaned[3], and Peerayot Sanposh[4*]

[1,2,3,4]Department of Electrical Engineering, Faculty of Engineering, Kasetsart University, Bangkok, Thailand
(Tel: +66-2-797-0999; E-mail: [1]watchara.hfs@gmail.com, [2]fengpyl@ku.ac.th, [3]fengnwc@ku.ac.th, [4]peerayot.s@ku.ac.th)
*Corresponding author: peerayot.s@ku.ac.th

Abstract: This paper presents a fractional integral terminal sliding mode control (FITSMC) for speed tracking of a DC motor employed in phenotyping robots for green environment applications. Phenotyping robots require high-precision motion control to ensure reliable and repeatable measurements of plants under field conditions where mechanical and load disturbances exist. To address these challenges, the proposed FITSMC ensured finite-time convergence of speed-tracking errors, even in the presence of unknown disturbances and modeling uncertainties. Unlike conventional sliding mode control, the FITSMC enables faster and more accurate convergence without requiring infinite control effort near the origin. Simulation results confirm the effectiveness and robustness of the proposed method, highlighting its potential for implementation in green robotic systems for precision agricultural applications.

Keywords: DC Motor, Finite-Time Control, Fractional Integral Terminal Sliding Mode Control (FITSMC), Phenotyping Robot.

1. INTRODUCTION

Plant phenotyping is a critical component of modern precision agriculture, where the accurate measurement of plant traits such as height, leaf area, and canopy structure plays a pivotal role in crop breeding and stress analysis [1]. Phenotyping robots—platforms equipped with sensors and actuators—have emerged as a powerful solution to automate and accelerate the phenotyping process in both greenhouse and field environments. A key requirement for phenotyping robots is that they must be able to execute precise and stable motion trajectories despite the presence of nonlinear dynamics, disturbances, and uncertain operating conditions.

DC motors are popularly used as actuators in phenotyping robots due to their simplicity, cost-effectiveness, and ease of control. However, DC motor dynamic behavior is often affected by modeling uncertainties and disturbances. These effects can degrade control performance and compromise the reliability of phenotyping data.

To address these challenges, sliding mode control (SMC) has been widely explored due to its robustness to uncertainties and disturbances [2], [3]. However, conventional SMC may have slow convergence. To overcome this drawback, fractional integral terminal sliding mode control (FITSMC) has been proposed as an advanced alternative. FITSMC combines integral sliding mode control (ISMC) and terminal sliding mode control (TSMC), incorporating the integral of a fractional power of the tracking error into the sliding surface [4]. Since the DC motor speed control system has a relative degree of one, ISMC is chosen. Additionally, TSMC introduces a nonlinear sliding surface that ensures finite-time convergence, compared to conventional SMC, while maintaining robustness against system uncertainties. In this study, we investigate the application of FITSMC for DC speed motor control in a phenotyping robot. A system identification process was conducted on a real DC motor, and the identified model was used to simulate the proposed control strategy. The robotic platform architecture, including the mechanical design, was developed by our research team, with a focus on field deployment for plant phenotyping robots. While real-time implementation is planned for future work, the simulation results show the effectiveness of the FITSMC in achieving accurate tracking and robustness to disturbances, confirming its potential for deployment in agricultural robotics.

Fig. 1 Phenotyping robot designed for precision agriculture, developed by our research group.

This article is organized as follows: Preliminaries on the DC motor model and finite-time control are introduced in Section 2. The FITSMC design is proposed in Section 3. In Section 4, our DC motor, its hardware, and system identification are presented. Simulation and results are discussed in Section 5. Section 6 concludes this paper.

† Watchara Jamnuch is the presenter of this paper.

2. PRELIMINARIES

2.1. DC Motor Model

2.1.1. Transfer Function Model

The behavior of a PMDC motor is governed by four equations: electrical, back electromotive force (EMF) voltage, torque generation, and mechanical equations [5]. These equations are given by:

$$v_a = R_a i_a + L_a \frac{di_a}{dt} + e_a \tag{1}$$

$$e_a = K_b \omega_m \tag{2}$$

$$T_m = J_m \frac{d\omega_m}{dt} + B_m \omega_m + T_L \tag{3}$$

$$T_m = K_t i_a \tag{4}$$

where v_a denotes the input armature voltage (V), e_a denotes the back EMF voltage (V), i_a is the armature current (A), ω_m represents the angular velocity (rad/s), T_m is the electromagnetic torque (N·m), R_a is the armature resistance (Ω), L_a is the inductance of the armature (H), J_m is the moment of inertia (kg·m^2), B_m is the viscous damping coefficient (N·m·s/rad), K_t is the torque constant (N·m/A), and K_b is the back EMF constant (V·s/rad),

The transfer function from the input voltage to the angular velocity is expressed by:

$$\frac{\omega_m(s)}{V_a(s)} = \frac{K_t}{(L_a s + R_a)(J_m s + B_m) + K_t K_b} \tag{5}$$

Since the electrical time constant L_a/R_a is much smaller than the mechanical time constant J_m/B_m, the armature inductance L_a can be neglected. The transfer function in Eq. (5) is simplified to:

$$\frac{\omega_m(s)}{V_a(s)} = \frac{K_t}{(R_a J_m)s + (R_a B_m + K_t K_b)} \tag{6}$$

2.1.2. State-Space Model

The state-space model of the PMDC motor can be expressed as:

$$\dot{\omega}_m = a\omega_m + b v_a - \frac{T_L}{J_m} \tag{7}$$

where

$$a = -\left(\frac{K_t K_b}{J_m R_a} + \frac{B_m}{J_m}\right) \tag{8}$$

$$b = \frac{K_t}{J_m R_a} \tag{9}$$

Let $a = a_0 + \Delta a$ and $b = b_0 + \Delta b$ where a_0, b_0 are the nominal values, and $\Delta a, \Delta b$ are the variations from parametric uncertainties. Consequently, Eq. (7) can be written as follows:

$$\dot{\omega}_m = a_0 \omega_m + b_0 v_a + d \tag{10}$$

where $d = \Delta a\, \omega_m + \Delta b\, v_a - T_L/J_m$ can be viewed as a disturbance from the parametric uncertainties and load torque.

Assumption 1: The disturbance $d(t)$ is bounded by a positive number Δ_{max}, i.e. $|d(t)| \leq \Delta_{max}$. ■

2.2. Finite-Time Control

Consider the nonlinear system given by:

$$\dot{s}(t) = f(t, s(t)),\ s(0) = s_0 \tag{11}$$

where $s \in \mathbb{R}^n$ is the system state, and $f : \mathbb{R}^+ \times \mathcal{D} \to \mathbb{R}^n$ is locally Lipschitz continuous with $f(t, 0) = 0, t > 0$.

Lemma 1: [6] Assume that there exists a continuously differentiable, positive definite function $V(s)$ on an open neighborhood $\mathcal{U}_0$ of the origin such that:

$$\dot{V}(s) \leq -\gamma V^{\alpha}(s),\ \forall s \in \mathcal{U}_0 \tag{12}$$

where $\gamma > 0$ and $0 < \alpha < 1$. Then, the origin is finite-time stable, and the reaching time is finite and satisfies the following inequality:

$$t_r(s_0) \leq \frac{1}{\gamma(1-\alpha)} V^{1-\alpha}(s_0) \quad \blacksquare \tag{13}$$

3. CONTROLLER DESIGN

3.1. Fractional Integral Terminal Sliding Mode Control

The FITSMC method is presented to achieve the speed tracking problem, i.e.,

$$\lim_{t \to \infty} \omega_m(t) = \omega_m^r(t), \tag{14}$$

where $\omega_m^r(t)$ is a reference trajectory. Therefore, let the tracking error be defined as:

$$e(t) = \omega_m^r(t) - \omega_m(t) \tag{15}$$

The FITSMC method is selected since the state-space model of the motor has the relative degree of one when the angular velocity is considered as the output.

The FITSMC is defined by the sliding variable as follows:

$$s(t) = e(t) + c \int_0^t e^{q/p}(\tau) d\tau, \tag{16}$$

where $c > 0$ is the integral gain and p, q are odd integers satisfying $p > q > 0$.

Remark 1: [6] If the system is on the sliding surface: $s(t) = 0, \forall t \geq t_0$ with initial tracking error $e(t_0) = e_0$, the tracking error $e(t)$ converge to zero in finite settling time t_s given by:

$$t_s(e_0) = \frac{|e_0|^{1-q/p}}{c(1-q/p)} \quad \blacksquare \tag{17}$$

To find the control v_a, the reaching law is selected as:

$$\dot{s} = -\varepsilon\, \mathrm{sgn}(s),\ \varepsilon > 0 \tag{18}$$

This law is known as the constant-rate reaching law [7]. The parameter ε determines how fast it reaches the sliding surface.

By differentiating Eq. (16), we obtain:

$$\begin{aligned} \dot{s} &= \dot{e} + c e^{q/p} \\ &= [\dot{\omega}_m^r - \dot{\omega}_m] + c e^{q/p} \end{aligned} \tag{19}$$

By substituting $\dot{\omega}_m$ from Eq. (10) and $\dot{s}$ from Eq. (18) into Eq. (19), we have:

$$-\varepsilon \operatorname{sgn}(s) = [\dot{\omega}_m^r - (a_0\omega_m + b_0 v_a + d)] + ce^{q/p} \quad (20)$$

Solving for v_a, we obtain:

$$v_a = \frac{1}{b_0}\left[\dot{\omega}_m^r - a_0\omega_m + ce^{q/p} + \varepsilon \operatorname{sgn}(s) - d\right] \quad (21)$$

Since all quantities on the right-hand side of Eq. (21) are known except the disturbance d, the control law in Eq. (21) cannot be implemented.

Consequently, by using the bound of d, the FITSMC is designed as follows:

$$\begin{aligned} v_a &= \frac{1}{b_0}\Big[\dot{\omega}_m^r - a_0\omega_m + ce^{q/p} + \varepsilon \operatorname{sgn}(s) \\ &\qquad + \Delta_{max} \operatorname{sgn}(s)\Big] \\ &= \frac{1}{b_0}\left[\dot{\omega}_m^r - a_0\omega_m + ce^{q/p} + k \operatorname{sgn}(s)\right] \end{aligned} \quad (22)$$

where $k = \varepsilon + \Delta_{max}$ is the FITSMC gain.

3.2. Stability Analysis

Theorem 1: Under the assumptions of bounded disturbances and model uncertainties, the FITSMC given in Eq. (22) ensures that the tracking error converges to zero in a finite time. The closed-loop system is stable in the sense of Lyapunov, and the reaching time is finite, provided that $k > \Delta_{\max}$. ■

To prove Theorem 1, consider the following candidate Lyapunov function:

$$V(s) = \frac{1}{2}s^2 \quad (23)$$

The derivative of $V(s)$ is given by

$$\begin{aligned} \dot{V} &= s\dot{s} \\ &= s\left([\dot{\omega}_m^r - (a_0\omega_m + b_0 v_a + d)] + ce^{q/p}\right) \end{aligned} \quad (24)$$

By substituting v_a from Eq. (22) into Eq. (24), we have:

$$\dot{V} = s\left(-k \operatorname{sgn}(s) - d\right) = -k|s| - ds \quad (25)$$

From Assumption 1, $-ds \le |ds| = |d||s| \le \Delta_{max}|s|$. Consequently,

$$\dot{V} \le -(k - \Delta_{max})|s| = -\gamma V^{1/2} \quad (26)$$

where $\gamma = \sqrt{2}(k - \Delta_{max})$. According to Lemma 1, $\gamma > 0$, or equivalently, the controller gain k must satisfy $k > \Delta_{max}$ to guarantee finite reaching time t_r, which is given by Eq. (13).

Consequently, since the settling time t_s, given by Eq. (17), is finite, the convergence time—equals the sum of t_r and t_s—is also finite. ■

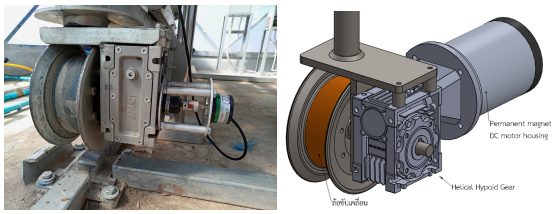

Fig. 2 DC motor mounted on the robot chassis along with its corresponding drive wheel.

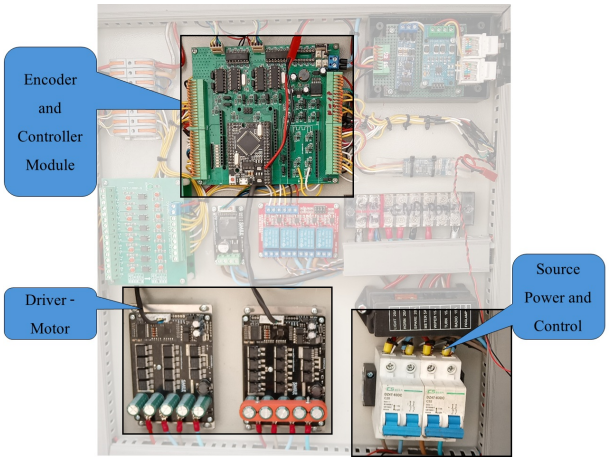

Fig. 3 Hardware of motor controller developed by our research group

4. SYSTEM IDENTIFICATION OF DC MOTOR

4.1. Hardware Design

Fig. 1 shows our phenotyping robot, which is designed to support high-precision motion control and modular sensor integration. The robot is designed to operate autonomously along predefined paths between crop rows, capturing plant phenotypic traits, such as height, leaf area, and canopy density, using onboard sensors.

Two DC motors, equipped with optical encoders, are used for locomotion, providing the position and velocity feedback necessary for closed-loop control. The frame is designed to minimize weight while maintaining sufficient structural rigidity for field conditions. Fig. 2 shows one of the DC motors mounted on the robot chassis along with its corresponding drive wheel.

The motor control system incorporates a feedback mechanism using encoders with differential signaling, ensuring robustness against signal interference. A custom-designed PCB facilitates this application, featuring electrical isolation between control and power drive circuits to minimize noise. The control board generates Pulse Width Modulation (PWM) signals, which are transmitted to the motor driver board for precise motor operation. The hardware layout is shown in Figure 3.

4.2. System Identification

4.2.1. Data collection

Since the wheel and motor do not have a predefined transfer function, it is necessary to determine the transfer function by measuring the motor speed in response

to a step-input voltage. The wheel is primarily driven by the motor, making the motor's transfer function a significant element. The first-order motor transfer function will be used to simplify the analysis, given that the input frequency is relatively low ($< 1\,\text{kHz}$). Other dynamics are treated as uncertainties, which are used to develop a robust control strategy.

Data collection for deriving the transfer function involves recording the motor's rotational speed as a function of voltage at 20 levels, sampled every 2 milliseconds over 60 seconds. This duration ensures the motor reaches steady-state conditions under no-load conditions for safety. The recorded data is then processed in MATLAB to observe the response. Signal processing techniques, such as Euler Backward differentiation and outlier detection and removal, are employed to filter out noise and remove anomalous data points. Finally, the cleaned data is used in the system identification process to extract a representative model for further use.

4.2.2. Motor Parameters

The transfer function is derived using the System Identification Toolbox in MATLAB. From the transfer function and the specification of the DC motor, the motor parameters are as follows: K_t = 0.0712; K_b = 0.0712; R_a = 0.2022; J_m = 0.082; B_m = 0.569.

5. RESULTS AND DISCUSSION

To evaluate and compare the effectiveness of FITSMC, three controllers are used. These controllers are given by:

1. PID Controller:

$$v_a = L^{-1}\left\{\left[K_p + \frac{K_i}{s} + K_d\frac{N}{1+N/s}\right]E(s)\right\} \tag{27}$$

where $K_p = 500$, $K_i = 1,000$, and $K_d = 3.4023$, $N = 1$.

2. ISMC:

$$v_a = \frac{1}{b_0}\left[\dot{\omega}_m^r - a_0\omega_m + ce + k\tanh\left(\frac{s}{\epsilon}\right)\right] \tag{28}$$

where $c = 400$, $k = 20$ and $\epsilon = 0.1$.

3. FITSMC:

$$v_a = \frac{1}{b_0}\left[\dot{\omega}_m^r - a_0\omega_m + ce^{q/p} + k\tanh\left(\frac{s}{\epsilon}\right)\right] \tag{29}$$

where $c = 400$, $k = 20$, $p = 5$, $q = 3$ and $\epsilon = 0.1$.

All controller parameters were tuned using particle swarm optimization (PSO), with the integral of absolute error (IAE) selected as the objective function. Notably, the signum function is replaced with the hyperbolic tangent function in both ISMC and FITSMC to mitigate chattering effects.

The following performance indices are used for evaluating the speed tracking performance of each controller:

1. Integral square error (ISE)
2. Integral absolute error (IAE)
3. Integral time absolute error (ITAE)
4. Max absolute error (MaxAE)

Fig. 4 compares the angular velocity responses of the PID, ISMC, and FITSMC controllers with the desired reference trajectory. Tracking errors and absolute values of tracking errors are shown in Figs. 5 and 6.

Table 1 Performance Metrics: ISE, IAE, and ITAE

Controller	ISE	IAE	ITAE
PID	0.000264	0.027921	0.054585
ISMC	0.000001	0.000752	0.001238
FITSMC	0.000000	0.000204	0.000349

Table 2 MaxAE

Controller	MaxAE (rad/s)
PID	0.016935
ISMC	0.005568
FITSMC	0.001587

As shown in Tables 1 and 2, the FITSMC controller achieves the best tracking performance among the three controllers evaluated, followed by ISMC, while the PID controller demonstrates the poorest performance. Moreover, FITSMC exhibits the least fluctuation in peak values and oscillatory behavior. These results suggest that FITSMC is well-suited for applications requiring high precision and actuator protection, such as agricultural phenotyping robots.

6. CONCLUSION

This paper presents a FITSMC for precise motion control of the DC motor used in the phenotyping robot platform developed by our team for green and sustainable agricultural applications. The proposed controller ensures finite-time convergence of the tracking error, offering enhanced robustness and fast response. The system identification process was conducted on our DC motor. Then, the resulting model was used to validate the control performance in a simulation environment. The simulation results confirm that the FITSMC approach achieves accurate angular velocity tracking under model uncertainties and external disturbances.

Future work will focus on real-time implementation of the proposed controller on our physical robot platform, along with field testing under realistic agricultural conditions and dynamic environments.

ACKNOWLEDGMENT

This project is supported by Precise Corporation Public Company Limited (PCC) and Program Management Unit for Competitiveness (PMUC), Office of National Higher Education Science Research and Innovation Policy Council, under Grant No. C10F640207. This work was carried out as part of the Master's Degree Program in the Department of Electrical Engineering, Faculty of Engineering at Kasetsart University.

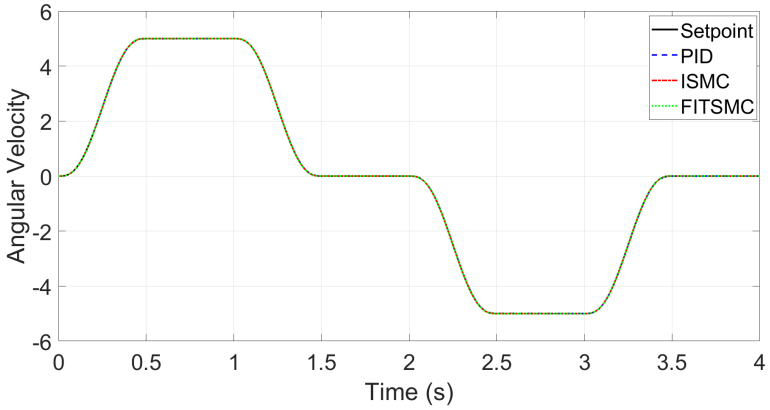

Fig. 4 Angular velocity (rad/s).

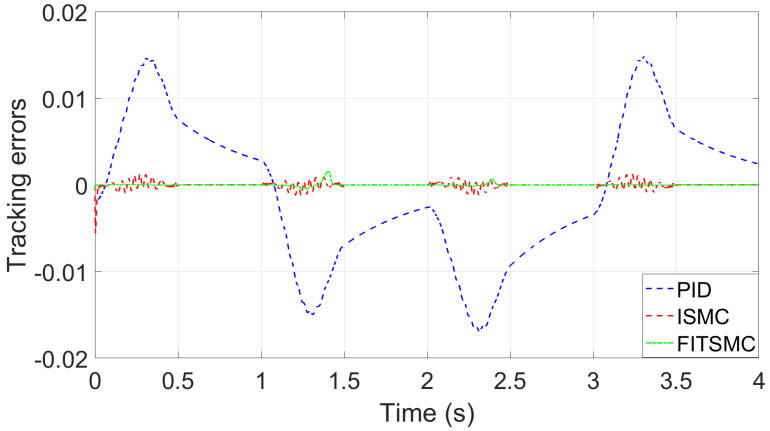

Fig. 5 Tracking errors (rad/s).

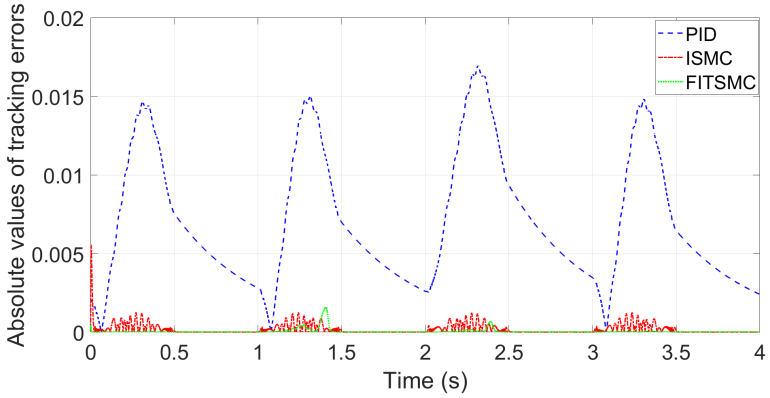

Fig. 6 Absolute values of tracking errors (rad/s).

REFERENCES

[1] A. Atefi, Y. Ge, S. Pitla, and J. Schnable, "Robotic technologies for high-throughput plant phenotyping: Contemporary reviews and future perspectives," *Frontiers in Plant Science*, vol. 12, pp. 1–17, Jun. 2021.

[2] V. Utkin, "Variable structure systems with sliding modes," *IEEE Transactions on Automatic Control*, vol. 22, no. 2, pp. 212–222, Apr. 1977.

[3] J. Liu and X. Wang, *Advanced Sliding Mode Control for Mechanical Systems: Design, Analysis and MATLAB Simulation*. Beijing, China / Berlin, Germany: Springer-Verlag Berlin Heidelberg and Tsinghua University Press, 2012.

[4] C.-S. Chiu, "Derivative and integral terminal sliding mode control for a class of mimo nonlinear systems," *Automatica*, vol. 48, no. 2, pp. 316–326, Aug. 2012.

[5] N. S. Nise, *Control Systems Engineering*, 7th ed. Hoboken, NJ, USA: John Wiley & Sons, 2015.

[6] Y. Liu, H. Li, Z. Zuo, X. Li, and R. Lu, "An overview of finite/fixed-time control and its application in engineering systems," *IEEE/CAA Journal of Automatica Sinica*, vol. 9, no. 12, pp. 2106–2120, Dec. 2022.

[7] K. Li, J. Ding, X. Sun, and X. Tian, "Overview of sliding mode control technology for permanent magnet synchronous motor system," *IEEE Access*, vol. Multidisciplinary, pp. 1–10, May 2024.